Chapter 3

Advanced Technologies for Large-Sized OLED Display

Chang Wook Han, Hong-Seok Choi, Chanki Ha,
Hongjae Shin, Hyun Chul Choi and In Byeong Kang

Additional information is available at the end of the chapter

http://dx.doi.org/10.5772/intechopen.74869

Abstract

Five years have passed, since the first 55″ full high-definition (FHD) OLED TV fabricated on Gen 8.5 glass was successfully launched into the TV market. For the time being, the size of OLED TV became diverse from 55″ to 77″, and the resolution was doubled into ultrahigh definition (UHD). The brightness and color gamut were enhanced, while the lower power consumption was realized. Utmost picture quality and slim form factor of OLED TV as well as the improved performance have made OLED TV recognized as the best premium TV. In this chapter, we describe the recent progress in three key technologies, which enable such an enhancement of performance in OLED TV, i.e., oxide thin-film transistor (TFT) and white organic light-emitting diode (WOLED), compensation circuit, and method to compensate the nonuniformity of oxide TFTs, OLED devices, and luminance.

Keywords: OLED TV, oxide TFT, white OLED, compensation circuit

1. Introduction

Organic light-emitting diode (OLED) is a very promising display. OLED provides a major technological enhancement to displays and TVs, such as wide viewing angle, high contrast ratio, and extremely fast response times. Furthermore, OLEDs can be used to make thin-light displays, transparent displays, and rollable displays.

OLED is a type of display technology that makes it possible to achieve dark black levels from ultrathin screens while at the same time making TVs more efficient and eco-friendly. OLED technology actively eliminated parts containing hazardous substances such as Cd, Hg, InP, etc. In addition, self-luminous OLEDs removed the backlight, helping designers

achieve a lightweight and slim design that used less parts and attained greater resource efficiency and recycle rates [1].

LG commercialized 15-inch OLED TVs in 2009. The technologies to realize the TVs were RGB deposition technology using a shadow mask and thin film transistor (TFT) using low-temperature polycrystalline silicon. However, it was difficult to produce larger-sized OLED TVs with the same technology applied to 15-inch OLED TVs. The shadow mask is applied to the mass production of small-sized OLED displays, forming RGB subpixels. However, this method is not suitable for larger OLED displays due to sagging in metal mask and defects and color mixing due to misalignment between mask and glass substrate. Also, the development of TFT for large substrate was another important obstacle. We need to further improve reliability and production yield of TFT.

Recently, there are several breakthroughs in realizing large OLED TVs. The first one is to use white OLED as the light source and implement the color via color layer. When WOLED receives an electric current, it mixes two or three wavelengths of light and produces a white light. For RGB color, the color layer was used to filter the white light. WOLED can provide solutions for manufacturing processed on large-sized substrate [2, 3]. This technique does not require sophisticated metal mask taking into consideration the misalignment margin of pixel designs. In addition, due to good process yield and high productivity, the eight-generation glass substrate can be deposited to produce large-sized OLED TVs. The second is an oxide TFT that was developed intensively to meet the large backplane requirements for OLED TVs [4, 5]. Oxide TFT is also capable of processing on eighth-generation glass substrates because of its similarity to amorphous silicon TFT and may be compatible with TFT lines for LCDs in terms of production lines. By combining WOLED and oxide TFT that can be made from large substrate, larger OLED TVs can be produced with higher productivity and lower cost.

We commercialized 55-inch full HD (FHD) OLED TVs in the early 2013 [6]. And then in 2016, we launched not only 65-inch and 55-inch ultrahigh definition (UHD) OLED TVs but also 77-inch UHD OLED TVs. In this chapter, we will describe advanced technologies including oxide TFTs, WOLEDs, and compensation circuit and UHD OLED TV.

2. Oxide TFT technology

2.1. Overview of TFT structure

The structure of TFT is classified as top and bottom gate depending on the relative position of gate and active layer. Additionally, when the gate is on the same side of source/drain electrodes, it is called coplanar structure. Two types of oxide TFT structures are shown in **Figure 1**. Double-gate TFTs with both top and bottom gates are illustrated by **Figure 1(a)**. Gate and SD2 electrode function as a bottom and top gate, respectively. As the advantageous side, this structure was utilized to increase current flow and gets better output characteristics [7]. However, large parasitic capacitances between gates and source/drain metals are disadvantages, which are a big hurdle developing UHD OLED TV. Coplanar TFT was designed to reduce parasitic capacitance avoiding overlap between gate terminal and source/drain

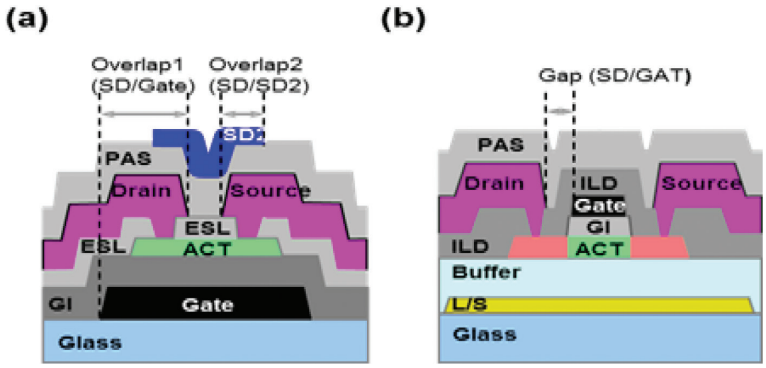

Figure 1. The cross-section of oxide TFT structures. (a) Etch-stopper structure with double gates and (b) self-aligned coplanar structure with top gate.

terminals as shown in **Figure 1(b)**. Light shield (LS) layer acts as blocking light coming to active layer, which is the main source to cause device degradation under negative bias temperature illumination stress (NBTIS). a-IGZO TFT with coplanar structure needs active metallization process to make ohmic contact between a-IGZO semiconductor and source/drain metals. This process was optimized to generate increased oxygen vacancies inside active film [8]. After metallization process, we obtained effective channel length, which is found to be shorter than nominal channel length. Effective channel length should be managed with controlled process.

2.2. Device characteristics

Driving TFTs for OLED TV operate in a current-driven mode, which control supplying current to OLED devices. Scan TFTs act as switches in active-matrix OLED (AM-OLED). It is important to obtain excellent device characteristics of these TFTs because device characteristics are directly connected to the performance and lifetime of OLED TV.

2.2.1. Electrical properties of a-IGZO TFT

Threshold voltage, subthreshold swing, field-effect mobility, and on/off current ratio can be extracted from I–V curve [9]. Typical values for each property are 0.5 V, 0.15 V/dec., 10㎠/Vs, and 10^7 at Vds = 10 V in the same order. Threshold voltage (Vth) is an important factor in the electrical characteristics, and it tells when the device turns on and off. Vth can be extracted from gate voltage when the drain current reaches 10 nA at the transfer curve under 10 V of drain voltage. Series resistance is also an important parameter in short-channel devices. The effective channel length can be obtained from the channel resistance method [10].

Figure 2(a) shows the transfer curves of 20pts TFTs located in six 55-inch panels which are fabricated on a Gen. 8.5 glass. The transfer curves were plotted by measuring the W/L = 26 μm/10 μm devices in the test element groups (TEG) through an inline probe station instrument. The inset picture shows the Vth distribution extracted from the real-time automatic Vth sensing instrument [11]. The variations of Vth extracted from transfer curve and automatic Vth sensing methods

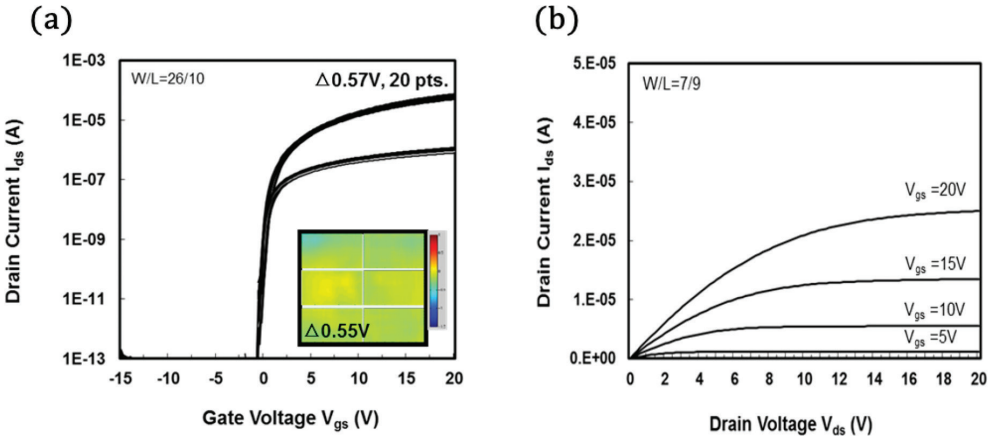

Figure 2. Transfer characteristic of a-IGZO TFTs on Gen. 8.5 glass (2200 × 2500mm).

were 0.57 V and 0.55 V, respectively. **Figure 2(b)** shows the output curves of the a-IGZO TFT. The output curve was plotted by sweeping the drain voltage from 0 V to 20 V, while gate voltages were applied from 5 to 20 V with 5 V steps.

Figure 3 is a graph plotting Rtot versus physical length of a-IGZO TFT with a width of 26 μm through the channel resistance method. ΔL, which is the difference between the physical channel length and the effective channel length of the coplanar a-IGZO TFT device, was calculated as 1.2 μm.

2.2.2. Reliability properties of a-IGZO TFT

Once OLED TV displays images, a-IGZO TFTs for OLED TV turn on and off repeatedly. In such operating environment, the device is stressed by continuous voltage, current, and temperature for a long time, which causes to degrade the electrical characteristics of a-IGZO TFT. The deteriorated a-IGZO TFT usually shows the change of Vth and drain current. This reduces the lifetime of

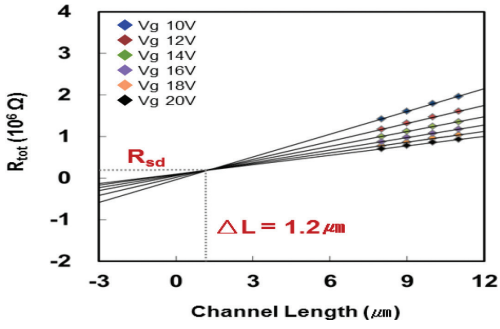

Figure 3. Illustration of the method used to extract effective channel length.

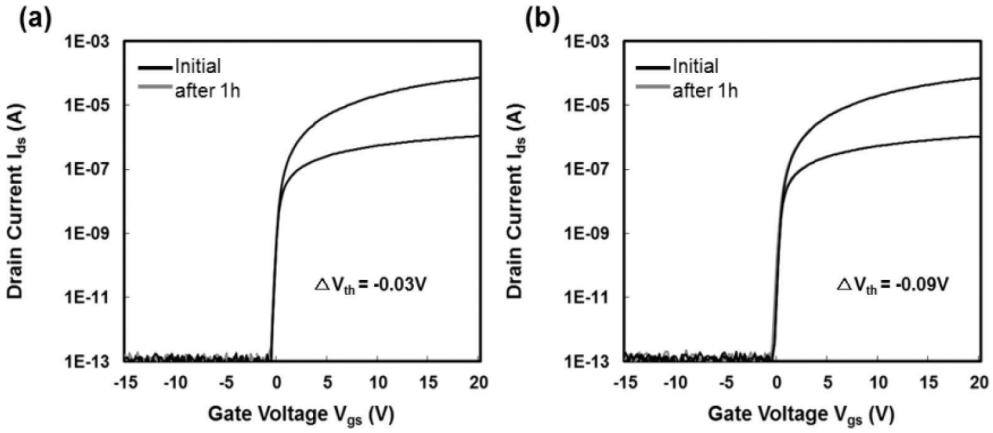

Figure 4. Shift of transfer curve after 1 h of negative gate bias at 60°C. Light emission from (a) top and (b) bottom.

the OLED TV or causes nonuniform luminance and image-sticking problems [12, 13, 14]. For this reason, a-IGZO TFT must be able to exhibit stable electrical characteristics for guaranteed lifetime. There are three typical methods to monitor device reliability such as NBTIS, positive bias temperature stress (PBTS), and current stress (CS) [15, 16, 17]. There are two well-known device degradation models of charge trapping in gate insulator [18] and defect creation in active layer models [19]. In addition, research has been going on the ambient effect model [20]. In order to improve the device reliability, it is necessary to optimize device fabrication process. Defect sites which are the source of charge trap should be reduced inside the oxide semiconductor thin film and at the interface between gate insulator and active layer. Studies have been conducted to improve device reliability. Oxide TFT was passivated to prevent external moisture and oxygen permeating into active layer [21, 22]. By applying light shield (LS) layer into TFT structure, it is possible to improve light-induced reliability degradation preventing active layer from the light [23].

Figure 4 shows the shift of transfer curve of a-IGZO TFT before and after NBTIS test. The NBTIS test was evaluated by applying Vgs = -30 V and Vds = 0 V at 60°C for 1 hour. The 4500 nit of visible light is also applied in the top and bottom directions of the device. **Figure 4** shows NBITS reliability characteristics of a-IGZO TFT under the top light (a) and bottom light (b). In both illumination tests, transfer curves shifted to the negative direction compared to the initial transfer curves. The amount of shifts was −0.03 V when top light was applied and − 0.09 V when bottom light was applied. It is believed that the amount of light is more injected into the device when the bottom light is illuminated than the top light.

3. WOLED and color filters

3.1. Two-stack tandem WOLED with two colors

WOLED employed to the first OLED TV launched in 2013 had a two-stack two-color tandem structure consisting of fluorescent blue and phosphorescent yellow-green (YG) stacks

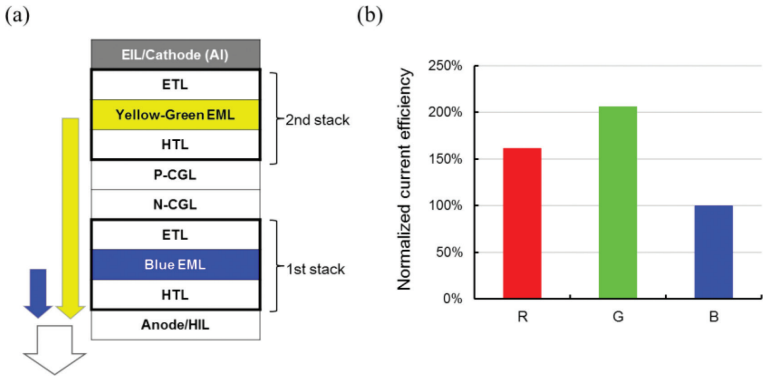

Figure 5. (a) Device structure of two-stack two-color tandem WOLED (b) relative current efficiency of red, green and blue subpixels normalized by the values needed to display full-window white pattern of 100 nit.

serially connected by n- and p-type charge generation layers, as shown in **Figure 5(a)** [2, 3, 24]. Specifications on luminance for the first OLED TV were 100 nit at full-window white pattern and 400 nit at peak-luminance pattern where 25% area is turned on. However, for the second models of OLED TV, 150 and 450 nit were demanded for the full-window and peak-luminance patterns, respectively, even at the lower power consumption.

Figure 5(b) shows relative current efficiencies (cd/A) of RGB subpixels after transmitting through color layer. These values are normalized by the efficiency for each subpixel, required to get a certain luminance. Since it is shown that blue subpixel is a restriction factor to the panel brightness, we need to drastically increase the efficiency of the blue device by more than 1.5 times. Two approaches could be considered in respect of external quantum efficiency and internal quantum efficiency. With regard to the external quantum efficiency, blue efficiency could be improved through a strong cavity effect using an electrode of thin metal. However, color shift varied by view angle could be worse. Regarding the internal quantum efficiency, phosphorescent blue [25, 26] or thermally activated delayed fluorescent (TADF) blue is still not around the corner.

3.2. Three-stack tandem WOLED with two colors

Our solution for the higher blue efficiency is three-stack tandem WOLED, namely, adding one more blue stack [27]. It is true that three-stack tandem WOLED needs higher applied voltage, which might become a factor to increase the power consumption. Nonetheless, three-stack WOLED can realize lower power consumption as well as higher luminance, which will be demonstrated later. As shown in **Figure 6**, three device architectures with different sequences of the unit devices are considered: (a) YG unit adjacent to the cathode (W1), (b) in the middle of the device (W2), and (c) adjacent to anode (W3). The best device architecture for three-stack two-color (3S2C) tandem WOLED is decided in terms of efficiency and color shift by viewing angle, with an assistance of optical simulation [28].

The viewing angle dependence of blue and YG efficiencies in each WOLED device can be predicted on the basis of the fact that angular dependence of blue and YG mono-devices is

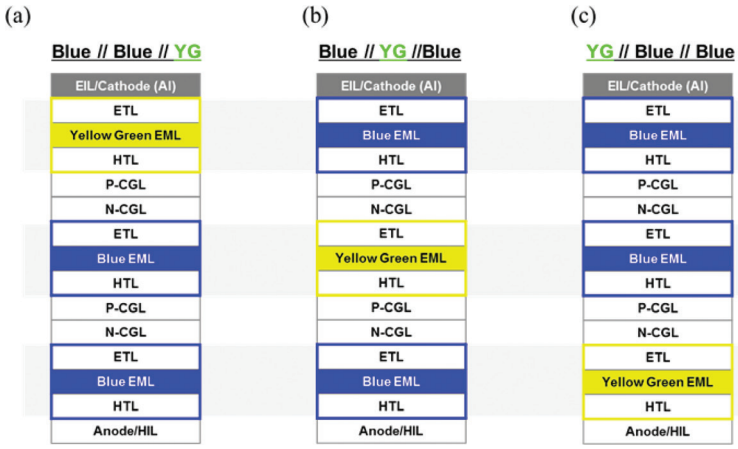

Figure 6. Three candidates for three-stack WOLED consisting of two fluorescent blue stacks and 1 phosphorescent YG stack.

correlated with the distance of EML from the cathode [27]. W1 whose both blue EMLs are farther from the cathode than YG EML shows that the blue intensity falls faster than the YG. W3 whose YG EML is farther from the cathode than the two blue EMLs shows that the YG intensity is reduced faster than the blue. In case of W2, as the blue intensities of two blue EMLs of which one is closer to and the other is farther from the cathode than YG EML, the blue efficiency is supposed to fall at the same trend with YG efficiency when the viewing angle is varied, resulting in little color shift. To comment on the viewing angle dependence of our two-stack WOLED depicted in **Figure 5(a)**, as blue EML is more distant from the cathode than YG EML, its color is supposed to shift toward YG at high incident angle.

We fabricated three-stack WOLED device where B, YG, and B units are sequentially formed, based on the optical simulation. **Table 1** summarized its actual performance compared with two-stack WOLED device. Since another blue device unit is supplemented, the voltage applied across the three-stack WOLED is enlarged by 4.5 V at the same current density of 10 mA/cm^2. However, the three-stack WOLED has the current efficiency (cd/A) enhanced by 8% and emits cool white light with high CCT of 8500 K, owing to its enhanced blue intensity by two blue units. Generally, TV panel displays white color with high CCT up to 9300~10,000 K. To realize such a cool white color using two-stack WOLED emitting white light of 6300 K CCT, the blue subpixel should be turned on with a high intensity, resulting in a high power consumption. The experimental electroluminance (EL) spectra varied by viewing angle, as depicted in **Figure 7(a)**, show that the intensities at blue and YG regions drop simultaneously at the same rate, resulting in very low color shift of 0.011 at 60°. The efficiency of blue subpixel for the three-stack WOLED is found to be enhanced by 75%, through adding one more blue stack, as shown in **Figure 7(b)**.

As mentioned above, the three-stack WOLED employing two stacks of blue device is advantageous to lowering the power consumption as well as boosting luminance of OLED panel.

	Two-stack WOLED	Three-stack WOLED
Voltage (V)	7.1	11.6
Efficiency (cd/A)	78.6	85.0
Color (Wx, Wy)	(0.317, 0.332)	(0.287, 0.310)
Color shift ($\Delta u'v'$)*	0.020	0.011

Table 1. The comparison of device characteristics between two-stack WOLED and three-stack WOLED at 10 mA/cm^2.

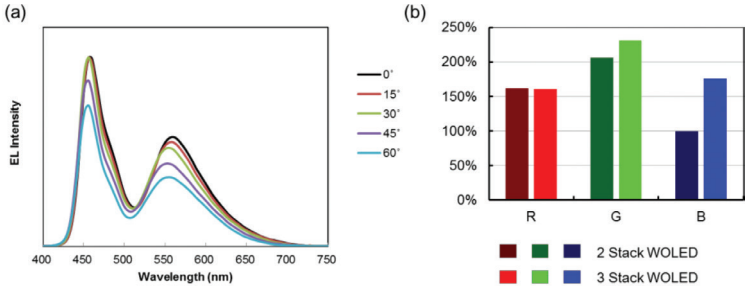

Figure 7. (a) Experimenal EL spectra of our real three-stack two-color tandem WOLED at various viewing angles showing that blue and YG intensities drop at the same ratio and (b) the comparison of efficiency of R, G, B subpixels between the two-stack tandem WOLED and three-stack tandem WOLED.

By enhancing the blue efficiency, the three-stack WOLED made our new OLED TV realize the luminance of 150 nit at full-window pattern which is higher by 50% compared to the first model using two-stack WOLED.

As regards to power consumption, we calculated time-average current values spent at each pixel of WRGB for OLED panels during playing a movie file ruled by the international standard CIE60287 at a fixed maximum luminance. The total current of OLED panel employing the three-stack WOLED is estimated to be at the 68% level of two-stack WOLED. Considering voltage rise of the three-stack WOLED, total voltage across WOLED and driving transistor in the backplane is increased by 10%. Namely, the final effect of the three-stack WOLED for saving the power consumption of OLED panel is calculated to be 24%.

To analyze the current of each subpixel in detail, OLED panel of the two-stack WOLED shows that a half of the total current is applied to the blue subpixel. In that case, by extending aperture ratio of the blue subpixel and lessening the current density, electrical stress on the blue subpixel could be reduced.

For the three-stack WOLED emitting cool white, red subpixel is more used to display warm colors, and the current to the red subpixel is slightly increased. However, the current decrease of blue subpixel as well as white subpixel is overwhelming. As a result, balancing of currents applied to four subpixels becomes better in the three-stack WOLED, which provides an advantage to OLED panel design. In addition, the lifetime for blue subpixel can be extended significantly.

3.3. Three-stack three-color tandem WOLED

The next urgent demand by our customers was to widen color gamut up to digital cinema initiatives (DCI) standard color space, after the luminance was enhanced by three-stack two-color (3S2C) tandem WOLED. The 3S2C WOLED has achieved 114% color gamut area compared to sRGB standard color but covered only 90% area in DCI standard color space [27]. In order to widen color gamut in DCI color space, deep green color with high CIE.y value and deep red color with high CIE.x value are necessary.

Since phosphorescent green EML did not show long enough lifetime for WOLED TV, we considered the insertion of an additional red EML in the three-stacked WOLED structure while maintaining the YG EML. By adding red EML, red color point was supposed to move toward higher CIE.x value. In case of green color point, we relied on optimizing green color layer.

As shown in **Figure 8**, considering contour map of the emittance [27, 28], three ways to add red EML in the three-stack WOLED could be taken into account. The two ways are as follows: a fluorescent red EML is added, adjacent to the fluorescent blue EML in the first- or third-stack unit. The other way is that a phosphorescent red EML is inserted, adjacent to the phosphorescent yellow-green in the second-stack layer. In the case of the three-stack three-color (3S3C) WOLED with fluorescent red EML, the blue EML in the third stack shares the exciton with the red EML so that the blue efficiency is decreased a little, but the overall efficiency (cd/A) is raised, thanks to the contribution of the red EML. As a result, the WOLED has warmer white. On the other hand, in the case of the WOLED with phosphorescent red EML, the YG EML in the second stack shares the exciton with the red EML. As the efficiency

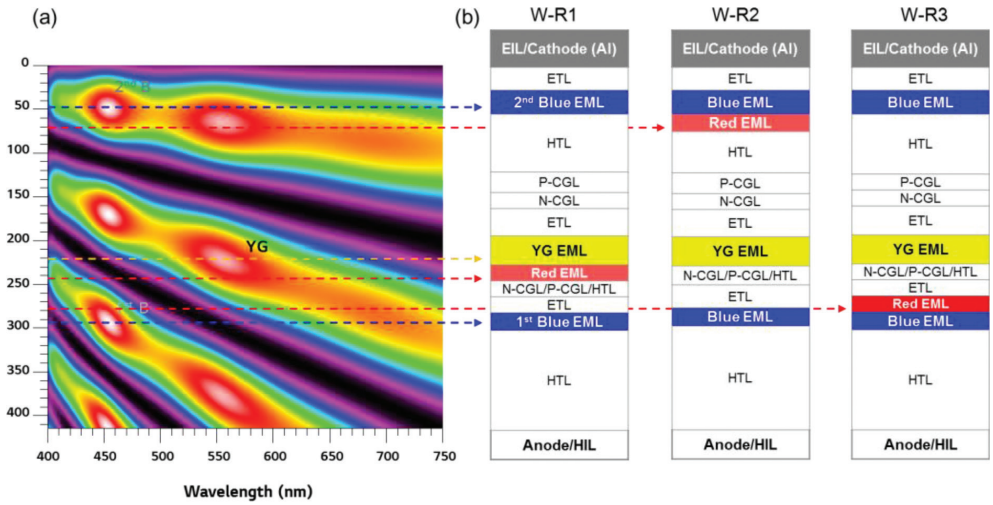

Figure 8. (a) Emittance contour map for three-stack three color tandem WOLED where red dotted lines are drawn at the position having relatively high emittance value near 620 nm. (b) Three device architectures for three-stack three color tandem WOLED; red EML in W-R1 is fabricaed before YG EML in the second stack, red EML in W-R2, before the second blue EML in the third stack, and red EML in W-R3, after the first blue EML in the first stack.

(cd/A) of the red EML is lower than that of the YG EML, this WOLED has the less efficiency than the 3S2C WOLED, but it emits the cool white light which is more suitable for the display application. Moreover, it is well known that fluorescent red materials do not show good lifetime performance. Thus, we should choose the WOLED involving the phosphorescent red (Ph-R) EML.

In the second case, or inserting phosphorescent R-EML, we fabricated a unit device of the phosphorescent red and YG (Ph-R/Ph-YG) EMLs whose structure is in the following, ITO/HTL/x% red dopant/12% YG dopant/ETL/EIL/Al, to examine the influence between red dopant ratio and YG dopant ratio. By controlling the concentration of R dopant at 12% YG dopant concentration, we obtained the best result at 2% R dopant concentration. **Figure 9(c)** illustrates EL spectra at the R doping ratio of 2 and 4% with the YG dopant fixed at 12% concentration. As R doping ratio is increased, the intensity in green region is reduced, and the intensity in red region is enhanced, while the external quantum efficiency (EQE) is slightly changed. These phenomena can be caused by the increase in the exciton energy transfer from YG EML to red EML owing to the increased red dopant concentration.

In addition to the red dopant concentration, it is also possible to control the relative intensities of red and green colors by changing the ratio of hole transport host and electron transport host in YG EML [3]. We have been adopting the mixed-host structure of a hole-type host and an electron-type host as a phosphorescent EML layer for high efficiency and long lifetime of WOLED. We fabricated Ph-R/Ph-YG unit devices along with the host ratio in YG EML of 0:10, 7:3, and 10:0 ratios of hole transport host and electron transport host at 12% YG dopant and 2% red dopant concentration.

Table 2 summarizes electrooptical performance of the Ph-R/Ph-YG unit devices, and **Figure 9(b)** shows EL spectra of the devices. When the hole-type host only (h-type host:e-type host =10:0) is used, the EL spectrum shows mainly YG peak with a slight red peak, which means that excitons were formed largely in the YG EML. As the ratio of the electron-type host in the YG EML is increased (h-type host:e-type host =7:3, 0:10), the YG peak

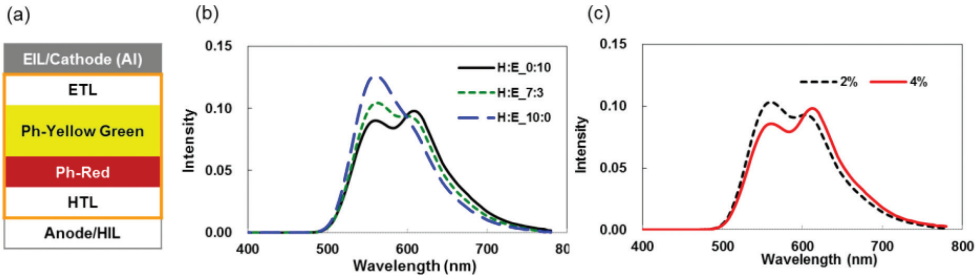

Figure 9. (a) Schematic diagram of phosphorescent unit device, (b) EL spectra of Ph-devices with different mixed host ratio at fixed YG and R dopant concentration, and (c) EL spectra of Ph-devices with the different R dopant concentration at fixed YG dopant concentration.

	Volt (V)	cd/A	EQE (%)	CIEx	CIEy
Host ratio (H:E)					
10:0	3.9	60.0	19.5	0.467	0.524
7:3	4.0	52.9	19.2	0.487	0.505
0:10	4.1	49.1	19.3	0.501	0.492
Red dopant Conc. (%)					
2	4.0	52.9	19.2	0.487	0.505
4	4.1	47.0	19.1	0.507	0.486

Table 2. Summary of device performance of Ph-devices (upper) with mixed host ratio at 10 mA/cm^2 (lower) with R dopant concentration at 10 mA/cm^2.

intensity is reduced, whereas the red peak intensity grows higher with approximately equal EQE. The increasing ratio of the electron-type host makes the facile electron transfer from YG EML to R EML. As a result, the electron-hole recombination zone will shift from the YG EML to the R EML/YG EML interface, which makes the rise of the R peak in the EL spectrum. We found the optimal spectrum at h-type host:e-type host = 7:3 ratio in YG EML. In case of Ph-R/Ph-YG unit device, we can control the red intensity with the host ratio as well as the dopant ratio.

There is an alternative way to increase the red intensity in WOLED, i.e., co-deposition of phosphorescent red and YG dopants at one EML in second unit device. Since the optimal doping ratio for the red dopant is in the range from 0.2 to 0.4%, the doping ratio should be precisely controlled. As the doping concentration of the red dopant was raised a little above the range, it was found that the intensity in green region is reduced, while the intensity in red region is increased. However, when the red doping ratio was too low, the exact ratio control between the red dopant and green dopant was not easy in process. Therefore, we considered inserting a red EML separately.

Figure 10(a) compares EL spectra of 3S3C and 3S2C WOLEDs. It found that 3S3C WOLED has distinct red peak at 620 nm and the higher red intensity than 3S2C WOLED, resulting in an efficiency enhancement of red subpixel by 38%. As shown in **Figure 10(b)**, EL spectrum at red subpixel after going through the red color layer (CL) is red-shifted by 10 nm. Consequently, by replacing 3S2C WOLED with 3S3C WOLED, color coordinates of the red subpixel are varied from (0.666, 0.332) to (0.678, 0.321), very close to the red chromaticity of the DCI standard, as depicted in **Figure 10(c)**. Regarding the color of the green subpixel, we obtained the high purity green color by developing a new green CL for high color gamut. Thanks to the new green CL, the color coordinates of the green subpixel were shifted from (0.300, 0.645) to (0.270, 0.666). As shown in **Figure 10(c)**, 3S3C WOLED with the new CLs covers most of the color space for the DCI standard, which corresponds to 99% color gamut of the DCI standard in CIE1976 (u'v') color space.

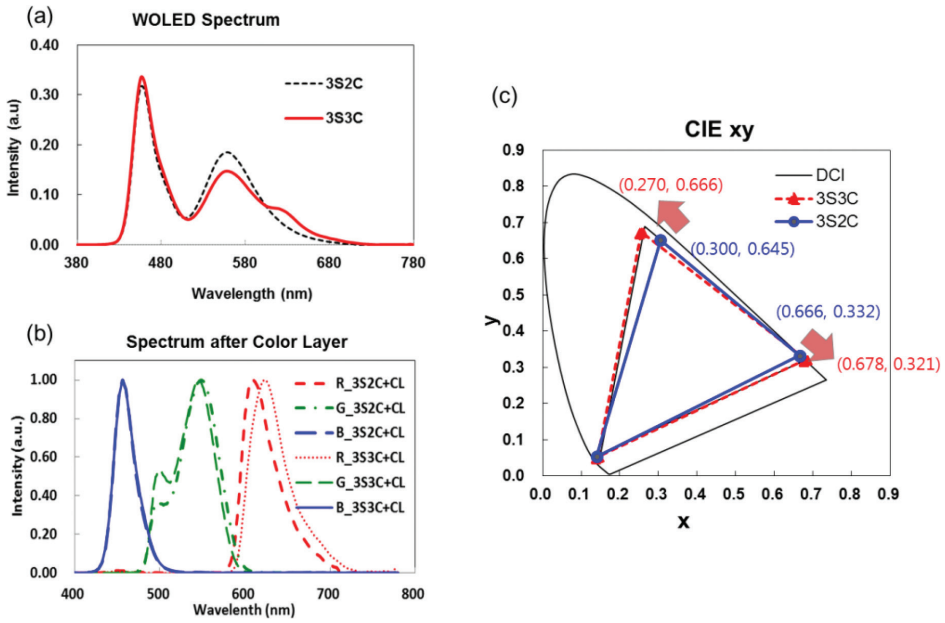

Figure 10. (a) Comparison of emission spectra of 3S2C and 3S3C WOLEDs (b) Emission spectra of 3S2C and 3S3C WOLEDs with color layers (c) Comparison of color gamut of 3S2C and 3S3C WOLEDs.

Table 3 summarizes the brightness and color gamut for 3S2C and 3S3C WOLEDs which are applied to OLED TV made in 2015 and 2016, respectively. As a result of such innovations in WOLED and CL, OLED TV could realize peak brightness of 500 nit and full-window brightness of 150 nit as well as high color gamut, i.e., 129% in sRGB color space and 99% in DCI color space.

	Year 2015	**Year 2016**
WOLED structure	3-stack 2-color (3S2C)	3-stack 3-color (3S3C)
Brightness (nit)	450/150	500/150
Color gamut (%)	sRGB 114%	sRGB 129%
	DCI 90%	DCI 99%

Table 3. The specification of OLED TVs based on 3S2C and 3S3C WOLEDs.

4. Compensation technologies

4.1. Pixel circuit

OLED displays, having current-driven subpixels, require higher backplane uniformity than LCDs. **Figure 11(a)** shows a simplified pixel circuit diagram of an active-matrix OLED display pixel.

Generally, the image data is supplied as a data voltage via a data line and applied to the gate of the driving transistor (DR) through the switching transistor (SW). The data voltage is stored in the storage capacitor (Cst), which keeps the gate-to-source voltage (Vgs) of DR stable even when the source voltage (Vs) changes according to the current–voltage characteristics of the OLED. The current flowing through DR is determined by Eq. 1:

$$I_{ds} = \frac{1}{2}\mu C_{ox}\frac{W}{L}\left(V_{gs} - V_{th}\right)^2 \quad (1)$$

The threshold voltage (Vth) determines the x intercept of the V–$I^{1/2}$ diagram of the transistor, while the mobility (μ), the capacitance per area of the gate insulator (C_{ox}), and the width-to-length ratio (W/L) determine the slope.

These values vary for each pixel because of fluctuations in layer thicknesses, etching biases, etc. and because of TFT degradations such as Vth shifts. The pixel current thus varies for each pixel as shown in **Figure 11(b)**. In order for an OLED display to achieve a high uniformity, the current variation must be compensated in each pixel.

4.2. Internal compensation and pixel circuit

OLED pixels with compensation traditionally employ additional TFTs, capacitors, and lines as in **Figure 12(a)**, which lowers the aperture ratio and increases defects [6], or power line voltage swinging as in **Figure 12(b)**, which is difficult to adopt in large-sized high-resolution panels because of large line loads and a short charging time. In order to achieve mass production of large-sized high-resolution OLED TVs, a simple pixel structure is necessary to reduce defects and improve aperture ratio [11]. Minimizing the number of TFTs in a subpixel can not only reduce defects but also simplify driving signals, which allows a narrow bezel design. We use a single data line and a single gate line for each subpixel, and the four subpixels in a full RGBW pixel share a sensing line and a power line, which reduces line crossings and thus reduces defects.

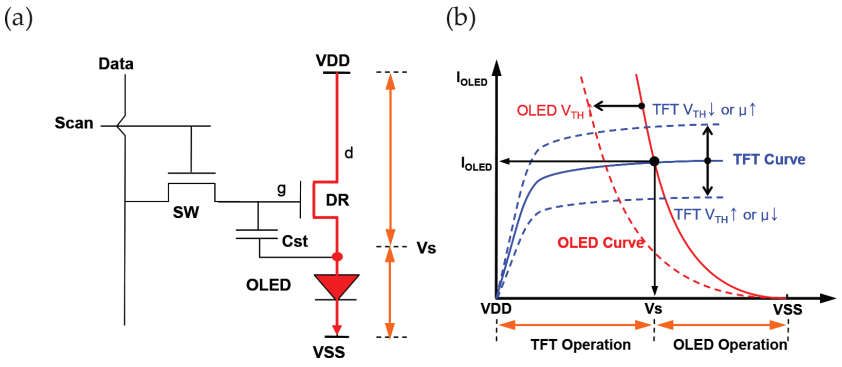

Figure 11. (a) OLED pixel circuit and operation voltages (b) OLED current at various TFT and OLED operation points.

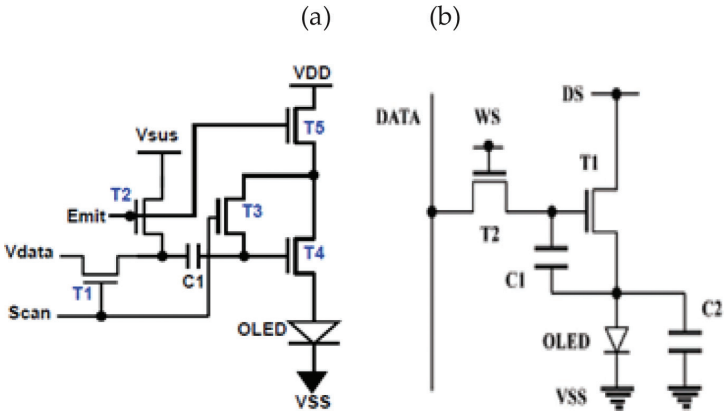

Figure 12. Internal compensation pixel circuits (a) 5T1C voltage programming (b) 2T2C voltage programming with VDD swing.

4.3. External compensation and pixel circuit

Figure 13 shows the concept of our external compensation [29]. From 2003, we developed LGD's unique compensation technology, including simple pixel structure, TFT compensation algorithm, and precise monitoring technology of TFT variation. Our pixel circuit satisfies UHD requirements such as a large screen, high compensation characteristics, and a high productivity. Our external compensation method compensates the threshold voltage and mobility variation of TFT. To get initial good uniformity of the luminance, compensation method is required to compensate variations of threshold voltage and mobility that cause luminance differences. Through the real-time sensing and compensation, our methods compensate threshold voltage shift and mobility shift.

Using this method, we solve reliability issues caused by positive and negative biases, temperature, and current stress. The subpixel itself does not have a compensation circuit, and the external circuit compensates each subpixel correctly. That makes the external circuit more complicated than internal compensation methods, because we need analog-digital converters, a sensing data memory, a compensation algorithm unit, etc. It has its own advantages: we can optimize compensation methods and parameters, not only for Vth but also for mobility, by using refined algorithms.

Figure 14 shows the sensing results of TFT Vth and mobility using external compensation pixel circuit. In our case, we sense the Vth and the mobility of the driving transistor in the source follower method shown in **Figure 14(b)**, where the data voltage for sensing (Vg) is applied to the gate of the driving transistor and the source voltage (Vs) is sensed by an external circuit. The difference between Vg and Vs is the Vth of the driving transistor and is stored to the memory. Using the sensed Vth, a Vth-compensated data voltage shown in Eq. 2 is applied to the gate:

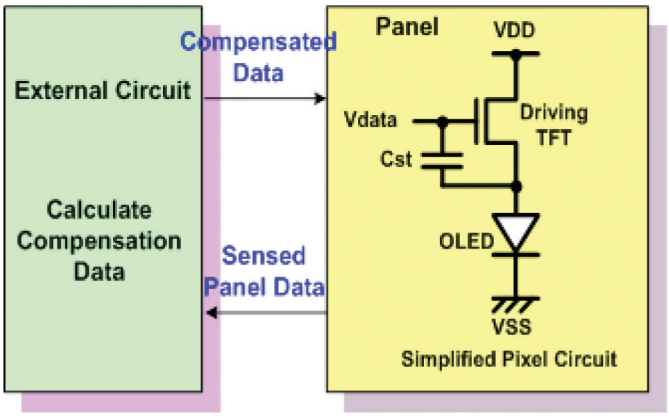

Figure 13. The external compensation method and the simplified pixel circuit.

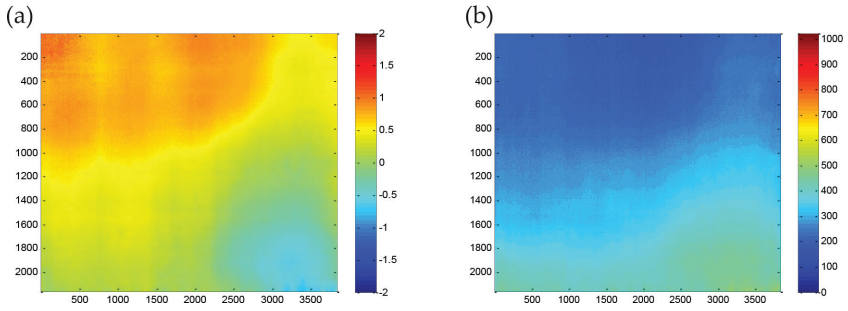

Figure 14. Sensing results of TFT (a) Vth and (b) mobility using extenal compenstion pixel circuit.

$$V'_{data} = V_{data} + V_{th} \tag{2}$$

Then, Vs is sensed, which is in proportion to the product of the TFT characteristics of the pixel except the Vth, which we call k here as shown in Eq. 3, where the capacitance of the sensing line (C_{line}) and the sensing time (t) are considered:

$$k = \frac{1}{2}\mu C_{ox}\frac{W}{L}V_{data}{}^{2}C_{line}t \tag{3}$$

Finally, by calculating the average of k of all pixels, we compensate each pixel by Eq. 4:

$$V'_{data} = \sqrt{\frac{k_{avg}}{k}}V_{data} + V_{th} \tag{4}$$

The pixel characteristics are sensed and compensated before shipment and in real time.

4.4. OLED degradation compensation

Other quality issues include image sticking. Firstly, being current-driven, OLED pixels generate heat when they emit light, and there may be a luminance change because of high temperature. Secondly, luminance will drop according to total driving time because of OLED degradation, like any other self-luminous device. For the former issue, we have designed a mechanical structure to release heat efficiently, and we use real-time temperature compensation. For the latter issue, we use a known correlation between current efficiency decrease and electric characteristic change of OLED [30]. OLED voltage–current characteristics change according to degradation, and we need a higher voltage to have the same current after OLED usage. We sense voltage for the same predetermined current to estimate OLED degradation at each subpixel and use a lookup table to translate OLED voltage shift to luminance compensation value. **Figure 15** compares time-dependent luminance curves for low stress and high stress, without and with repeated OLED voltage sensing and luminance compensation. Luminance difference can be minimized between high-stress and low-stress subpixels through the OLED degradation compensation. We sense OLED degradation with a predetermined interval because OLED degrades much slower than TFT. We do not compensate OLED luminance completely to maintain initial luminance, because OLED compensation rather accelerates degradation. Instead, we match OLED luminance to target degradation curve. **Figure 16(a)** shows the image sticking

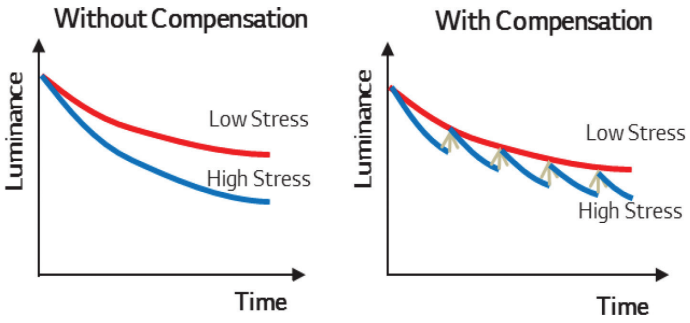

Figure 15. Image sticking compensation method due to OLED degradation.

Figure 16. Image sticking test results (a) Before compensation, (b) After compensation.

of the OLED panel due to OLED degradation. **Figure 16(b)** demonstrates the drastic disappearance of the image sticking after the OLED degradation compensation.

5. World's first UHD OLED TV products

Figure 17 is a photograph of the 55-, 65-, and 77-inch UHD OLED TVs, which are world's first products. These OLED TVs are employing TFT backplane composed of coplanar a-IGZO TFTs, three-stack three-color tandem WOLED and advanced compensation technologies. Our technology platform allows a panel size scalability, a product reliability, and a high aperture ratio. **Table 4** shows specifications of our UHD OLED TVs with high color gamut, high contrast ratio, and thin thickness.

The reason why OLED TV is known to have the best quality of display is that it realizes high contrast ratio since OLED at each subpixel can be completely and individually turned off by oxide TFTs when the subpixel displays zero signal. Low-leakage current of oxide TFTs contributes to the high contrast ratio of OLED TV. Namely, OLED TV can easily achieve high dynamic range (HDR) without raising up the peak luminance, contrary to LCD TV. Accordingly, OLED

Figure 17. Photograph of LG's 55-, 65- and 77-inch UHD OLED TV products.

Item	Content	Unit
Display type	WRGB OLED	
Panel size	55, 65, 77	inch
Resolution	3840 × 2160 (UHD)	
Brightness	150 (full)/500 (peak)	cd/m^2
Color gamut (DCI* coverage)	99 (DCI)	%
Contrast ratio	> 1000000:1	

Table 4. Specifications of the LG UHD OLED TV (*DCI: Digital Cinema Initiatives).

TV has an advantage to realize wide-span HDR with low power consumption. New compensation technologies can extend life span of OLED TV by relieving image sticking which seems inevitable for the spontaneous emission-type displays. The ultra-slim thickness of OLED TV not only offers premium values in view of design but also entitles OLED TV as green electronics by eliminating several plastic sheets in LCD TV.

6. Conclusion

In this chapter, we have explained the latest progresses in three key technologies, i.e., oxide TFT, WOLED, and advanced compensation circuit and method, applied to brand-new UHD OLED TV. a-IGZO TFTs with coplanar structure have demonstrated excellent electrical and reliability characteristics, which will be a good reference for the future development as well as for mass production of large-sized UHD OLED TVs. New device architectures of three-stack and/or three-color WOLED could realize OLED TV with high luminance and high color gamut. The advanced compensation technologies, including the external compensation method, have enabled a panel size scalability and an enhancement of the lifetime reliability necessary for commercializing large-sized and high-resolution OLED TVs.

Not to mention higher luminance and lower power consumption, OLED TV with higher resolution such as 8 K x 4 K, higher color gamut such as BT2020 and larger size than 80″ should be developed in the future. Although all these are definitely a huge challenge to oxide TFT, WOLED, and advanced compensation technology, it is believed that these will be realized via innovations and breakthroughs coming from momentum of research and development well established in these fields.

Author details

Chang Wook Han*, Hong-Seok Choi, Chanki Ha, Hongjae Shin, Hyun Chul Choi and In Byeong Kang

*Address all correspondence to: hcw@lgdisplay.com

LG Display, Seoul, Korea

References

[1] Kim S et al. Paper No S4.2: Eighth Generation Linear Source for AMOLED Mass Production. In: SID Symposium Digest of Technical Paper (EuroDisplay ‘15); 2015. p. 18

[2] Han CW et al. 21.2: 55-inch FHD OLED TV employing new tandem WOLEDs. In: SID Symposium Digest of Technical Papers (SID 12). 2012. pp. 279-281

[3] Han CW et al. 53.2: Invited Paper: Advanced Technologies for Large-sized OLED TV. SID Symposium Digest of Technical Papers (SID '14); 2014. pp. 770-773

[4] Nomura K et al. Room-temperature fabrication of transparent flexible thin-film transistors using amorphous oxide semiconductors. Nature. 2004;**432**:488-492. DOI: 10.1038/nature03090

[5] Yabuta H et al. High-mobility thin-film transistor with amorphous InGaZnO4 channel fabricated by room temperature rf-magnetron sputtering. Applied Physics Letters. 2006;**89**:112123. DOI: 10.1063/1.2353811

[6] Oh CH, Shin HJ, Nam WJ et al. Technological Progress and Commercialization of OLED TV. In: SID Symposium Digest of Technical Papers (SID '13); 2013. pp. 239-242

[7] Nag M et al. Characteristics improvement of top-gate self-aligned amorphous indium gallium zinc oxide thin-film transistors using a dual-gate control. Journal of the Society for Information Display. 2017;**25**:349-355. DOI: 10.1002/jsid.558

[8] Bae JU et al. Development of oxide TFT's structures. In: SID Symposium Digest of Technical Papers (SID '13). 2013. pp. 89-92

[9] Kagan CR, Andry P, editors. Thin-Film Transistors. New York: Marcel Dekker; 2003

[10] Sato A et al. Amorphous in-Ga-an-O coplanar homojunction thin-film transistor. Applied Physics Letters. 2009;**94**:133502. DOI: 10.1063/1.3112566

[11] Yoon JS et al. 55-inch OLED TV using optimal driving method for large-size panel based on InGaZnO TFTs. In: SID Symposium Digest of Technical Papers (SID 14). 2014. pp. 849-852

[12] Guo X et al. Investigation on the current nonuniformity in current-mode TFT active-matrix display pixel circuitry. IEEE Transactions on Electron Devices. 2005;**52**:2379-2385. DOI: 10.1109/TED.2005.857936

[13] Chaji GR et al. Electrical compensation of OLED luminance degradation. IEEE Electron Device Letters. 2007;**28**:1108-1110. DOI: 10.1109/LED.2007.909854

[14] In HJ et al. External compensation of nonuniform electrical characteristics of thin-film transistors and degradation of OLED devices in AMOLED displays. IEEE Electron Device Letters. 2009;**30**:377-379. DOI: 10.1109/LED.2009.2014885

[15] Suresh A et al. Bias stress stability of indium gallium zinc oxide channel based transparent thin film transistors. Applied Physics Letters. 2008;**92**:033502. DOI: 10.1063/1.2824758

[16] Oh H et al. Photon-accelerated negative bias instability involving subgap states creation in amorphous in–Ga–Zn–O thin film transistor. Applied Physics Letters. 2010;**97**:183502. DOI: 10.1063/1.3510471

[17] Nomura K et al. Comprehensive studies on the stabilities of a-In-Ga-Zn-O based thin film transistor by constant current stress. Thin Solid Films. 2010;**518**:3012-3016. DOI: 10.1016/j.tsf.2009.09.193

[18] Lee JM et al. Bias-stress-induced stretched-exponential time dependence of threshold voltage shift in InGaZnO thin film transistors. Applied Physics Letters. 2008;**93**:093504. DOI: 10.1063/1.2977865

[19] Nomura K et al. Origins of threshold voltage shifts in room-temperature deposited and annealed a-in-Ga-Zn-O thin-film transistors. Applied Physics Letters. 2009;**95**:013502. DOI: 10.1063/1.3159831

[20] Jeong JK et al. Origin of threshold voltage instability in indium-gallium-zinc oxide thin film transistors. Applied Physics Letters. 2008;**93**:123508. DOI: 10.1063/1.2990657

[21] Chen WT et al. Oxygen-dependent instability and annealing/passivation effects in amorphous in–Ga–Zn–O thin-film transistors. IEEE Electron Device Letters. 2011;**32**:1552-1554. DOI: 10.1109/LED.2011.2165694

[22] Li J et al. Effect of reactive sputtered SiOx passivation layer on the stability of InGaZnO thin film transistors. Vacuum. 2012;**86**:1840-1843. DOI: 10.1016/j.vacuum.2012.04.009

[23] Oh S et al. Suppression of light influx into the channel region of photosensitive thin-film transistors. IEEE Transactions on Electron Devices. 2015;**62**:4057-4062. DOI: 10.1109/TED.2015.2492680

[24] Han CW et al. 11.1: Invited paper: 15-inch RGBW panel using two-stacked white OLED and color filter for large-sized display applications. In: SID Symposium Digest of Technical Papers (SID '10). 2010. pp. 136-139

[25] Lee J et al. Deep blue phosphorescent organic light-emitting diodes with very high brightness and efficiency. Nature Materials. 2016;**15**:92-98. DOI: 10.1038/nmat4446

[26] Lee J et al. Hot excited state management for long-lived blue phosphorescent organic light-emitting diodes. Nature Communications. 2017;**8**:15566. DOI: 10.1038/ncomms15566

[27] Choi HS et al. 45.1: Invited paper: Recent progress of white light-emitting diodes for an application to new models of OLED TV. In: SID Symposium Digest of Technical Papers (SID '16). 2016. pp. 605-608

[28] Choi HS et al. Optimization of 2-stack WOLED structure with consideration on color gamut and power consumption. Journal of Display Technology. 2009;**5**(12):546-551. DOI: 10.1109/JDT.2009.2033822

[29] Jung SH et al. A new AMOLED pixel compensating the combination of n-type TFT and normal OLED device. In: SID Symposium Digest of Technical Papers (SID 09). 2009. pp. 1-4

[30] Shin HJ, Takasugi S, Park KM, et al. Technological progress of panel design and compensation methods for large-size UHD OLED TVs. In: SID Symposium Digest of Technical Papers (SID '14). 2014. pp. 720-723